

# Scanning Electron Microscopy

---

Volume 1985  
Number 1 1985

Article 28

---

11-26-1984

## Wave-Length Dispersive Microprobe Analysis of Coated Samples of Bulk Tissues

C. Ward Kischer  
*University of Arizona, Tucson*

Thomas M. Teska  
*University of Arizona, Tucson*

Follow this and additional works at: <https://digitalcommons.usu.edu/electron>



Part of the [Biology Commons](#)

---

### Recommended Citation

Ward Kischer, C. and Teska, Thomas M. (1984) "Wave-Length Dispersive Microprobe Analysis of Coated Samples of Bulk Tissues," *Scanning Electron Microscopy*: Vol. 1985 : No. 1 , Article 28.

Available at: <https://digitalcommons.usu.edu/electron/vol1985/iss1/28>

This Article is brought to you for free and open access by the Western Dairy Center at DigitalCommons@USU. It has been accepted for inclusion in Scanning Electron Microscopy by an authorized administrator of DigitalCommons@USU. For more information, please contact [digitalcommons@usu.edu](mailto:digitalcommons@usu.edu).



WAVE-LENGTH DISPERSIVE MICROPROBE ANALYSIS OF  
COATED SAMPLES OF BULK TISSUES

C. Ward Kischer\* and Thomas M. Teska

Department of Anatomy, College of Medicine\*, and  
Lunar and Planetary Laboratory  
University of Arizona, Tucson, AZ 85724

(Paper received February 21 1984, Completed manuscript received November 26 1984)

Abstract

Hypertrophic scars contain highly pleomorphic cells, including many from the erythrocytic series which have been extravasated. The conventional visual mode of SEM cannot distinguish the cell types with certainty except in the case of typical biconcave disc-shaped erythrocytes. Microprobe elemental analysis might be used to differentiate one type from another on the basis of iron and possibly phosphorus (for nucleated cells). Using coated specimens (gold or gold-palladium) precludes simultaneous visual mode SEM with EDX because of energy line interference with phosphorus and other elements. However, wave-length dispersive analysis offers minimal or no interference, and a coated specimen offers the use of a simultaneous visual mode. We wished to determine if useful elemental data could be obtained from specimens previously prepared only with the purpose of SEM mode studies. Therefore they were not prepared according to contemporary optimal methods. Analysis demonstrates that one group of cells contains 45% or more (dry weight concentration, absolute) iron as opposed to markedly low values in other cell types. Values for phosphorus do not appear essentially different among the cell types except in the case of standard erythrocytes where it is very low. Calcium and sulfur content was also examined. Sulfur might be useful in identifying another cell type in the hypertrophic scar. Using cells and matrix in developing deer antler for control values, the ratio of calcium to phosphorus found in the mineralizing matrix was essentially the predicted value. It is concluded, therefore, that even with a substantially heavy coating of gold, values for the elements tested (Fe, P, Ca, S) are not seriously compromised.

**KEY WORDS:** skin, hypertrophic scar, scanning electron microscopy, erythrocytes, myofibroblasts, wave-length dispersive analysis chondrocytes, collagen, mineralizing matrix

\*Address for correspondence:

C. Ward Kischer  
Department of Anatomy, College of Medicine,  
University of Arizona,  
Tucson, AZ 85724 Phone No.: (602) 626-6090

Introduction

Previous studies of human fibrotic lesions by the senior author using Scanning Electron Microscopy (SEM) (Kischer, 1974a,b; Kischer et al., 1975; Kischer & Shetlar, 1979) demonstrated pleomorphic cells which could not be accurately classified. Within the connective tissue of a hypertrophic scar or keloid many cells may have a considerable variability in shape. Erythrocytes which may be extravasated also show a wide range of deformation (Bessis, 1973). There is sufficient similarity between the altered forms of the cells that by SEM one has great difficulty in telling them apart. Transmission electron microscopy would most likely solve this problem. However, in the effort to avoid extensive processing and the addition of considerably more technique and handling we believed a method of elemental analysis using iron (Fe) and possibly phosphorus (P) might at least separate erythrocytic cell types from others.

Our specimens had previously been prepared for only the SEM mode of study. In order to identify cells for x-ray analysis they must be coated. Even though we used specimens already on hand, we did attempt some carbon coating alone but found this was insufficient to prevent charging, which prohibited our finding cells for study. Our specimens were coated with gold alone or a gold-palladium mixture. The coating of these specimens rendered extremely difficult, if not impossible, the energy dispersive system because of the overlap of energy lines between gold, phosphorus and sulfur.

Therefore, we used wave-length dispersive analysis (WDX) in conjunction with SEM. Our preliminary results show that WDX can be used with confidence on gold-coated bulk tissue samples for elemental analysis and may provide a useful means of separating certain cell types using iron, phosphorus or sulfur.

Using Med-Line search over the past seven years and a 1983 SEM Inc. publication (Basic Methods in Biological X-ray Microanalysis, Roomans & Shelburne, 1983) we found very few references which indicate that this kind of investigation using WDX had ever been done (Makita, 1981). If successful, this method might enable many researchers to make use of their

TABLE 1: WDS - SPECTROMETER AND CALIBRATION DATA

Element	Line	Crystal	Peak	Inten.	Bkg.	Inten.	Std.	c/ZAF	Au residual
Fe	K	LIF	1.9374	107	±.010	2.4	troilite	.5885	$0.1 \times 10^{-4}$
P	K	PET	2.8364	57	.012	1.5	apatite	.1680	-0.1
Ca	K	LIF	3.3595	88	.010	4.6	apatite	.3730	0.6
S	K	PET	2.4749	153	.010	4.4	troilite	.3519	1.5
Au	M	PET	2.6932	92	.035	1.5	Au100	1.000	---
Pd	L	PET	2.0118	66	.010	12	Au <sub>60</sub> /Pd <sub>40</sub>	.3485	---

Peak positions (Peak) and background offsets (Bkg.) are in A units for LIF geared spectrometers. Intensities (Inten) are in counts/second per nA of sample current. Relatively high background intensities result from the use of small offsets employed to avoid curvature effects which would otherwise occur during linear background interpolation. c/ZAF is the ZAF adjusted fraction of the element in the standard. Au residual is the spurious fraction measured on pure (99.99%) Au standard. 15 keV data. The diffracting crystals in the spectrometers are lithium fluoride (LIF) and pentaerythritol (PET).

many gold-coated specimens, once used only for visual mode scanning EM, for elemental analysis.

#### Materials and Methods

Hypertrophic scars, keloids or normal skin were obtained fresh from the operating room, or in the case of deer antler, from the velvet stage of annual replacement, fixed immediately in Karnovsky's fluid with cacodylate buffer for a minimum of one hour. They were hand cut with a stainless steel razor blade into pieces which varied from 1 to 5 mm thick and 2 to 8 mm wide. After washing in cacodylate buffer the pieces were dehydrated in a graded series of acetone, brought to absolute acetone from which they were transferred to a liquid CO<sub>2</sub> chamber and dried by the critical point method.<sup>2</sup> Specimens were coated either with gold or gold-palladium (60%-40%) with an intended thickness of approximately 200A to 600A of gold or gold-palladium. These specimens were on hand from SEM mode studies made previously.

We were interested in distinguishing erythrocytic cells from fibroblast types or others on the basis of iron content. Because the erythrocyte is a non-nucleated cell we also wished to examine the cells for phosphorus believing that the amount of this element might be higher in nucleated cells because of the phosphorus in the nucleotides.

The regenerating deer antler was studied because identification of nucleated cells (chondrocytes) was quick and easy.

We were also interested in analyses for calcium because of the nature of the myofibroblast (a contractile cell normally found in the scars) and for sulphur because of the

chondroitin sulfates in the connective tissue matrix of the scars.

Within the developing deer antler there is a relatively thick zone of myofibroblasts. Therefore, these cells were easy to locate and obtain data from; therefore, they also served as a control.

For control values for erythrocytes we obtained fresh blood samples from normal individuals, diluted an aliquot of unclotted blood with an equal volume of surgical Ringer's and placed several capillary drops on a spectrographically-pure carbon platform. After waiting a few seconds for settling of the cells and aspirating off most of the meniscus the platform was gently immersed in Karnovsky's fixative. This was followed by dehydration in graded alcohols and drying by the critical point method.

We used an Applied Research Laboratories Model SEMQ microprobe operated by a Tracor Northern automation and data reduction system. Four WDX spectrometers were available as well as energy dispersive detection capabilities (EDX) and essentially no effort was required to alternate between SEM and elemental analysis modes.

We operated at 15kV and 10nA sample current (30nA for the control erythrocytes), with untilted specimens so that the nominal x-ray take-off angle for all spectrometers would remain at 52.5 degrees. To achieve a desired minimum level of detectability, in the presence of a high background and weakened characteristic x-rays caused by the coating, we used 800 seconds counting time (peak plus background) plus shorter times to monitor the elements in

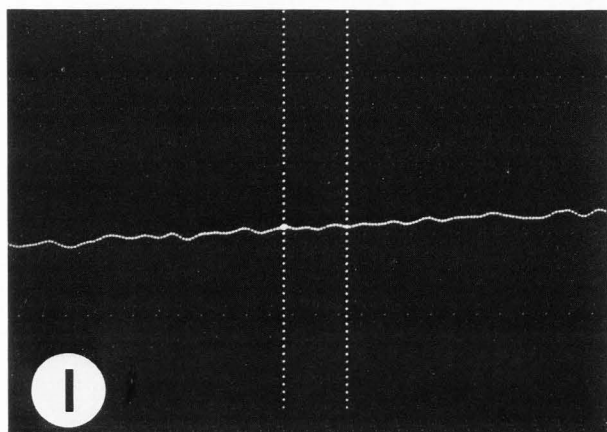


Fig. 1 Lithium fluoride (LIF) spectrometer scan centered on Fe K-alpha peak location, from +0.1 to -0.1 A (LIF). Bulk gold/palladium sample with 100nA current at 15kV. 200 points at 6 sec. per point. Vertical lines indicate background positions used. Subsequent measures indicate  $+0.1 \times 10^{-4}$  Au residual reported in Table 1.

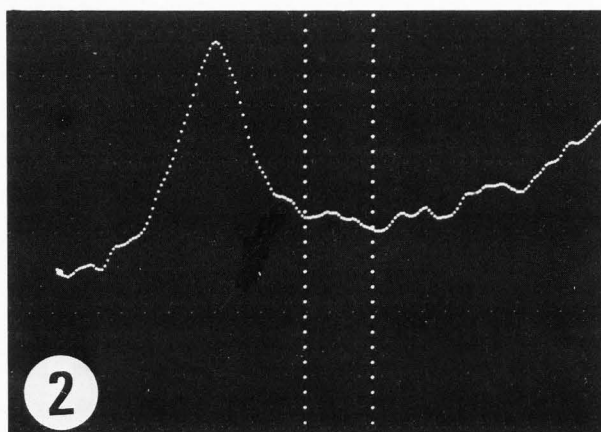


Fig. 2 Pentaerythritol (PET) spectrometer scan centered on P K-alpha peak location, as in Fig. 1. Background shift caused by the Au ( $M_3-N_1$ ) peak results in the  $-0.1 \times 10^{-4}$  Au residual in Table 1.

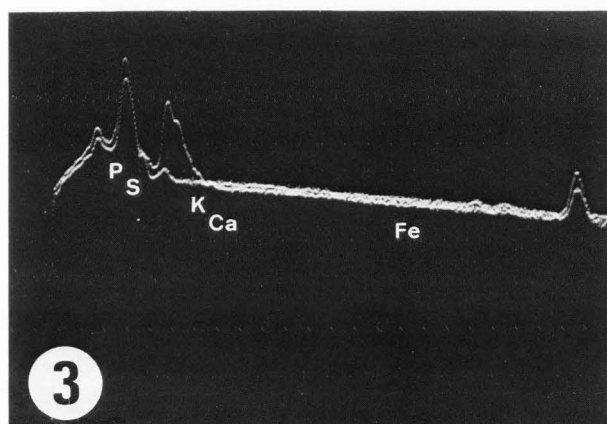


Fig. 3 Energy dispersive spectra (EDS), 1 to 10 keV, of coating materials. Superimposed gold and gold60/palladium40. Locations for peaks of interest in this study are marked. Logarithmic vertical scale.

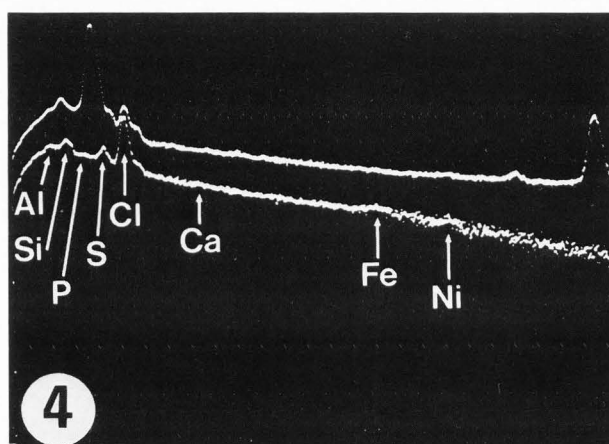


Fig. 4 EDS spectra, 1 to 10 keV, of erythrocyte on carbon stub. Superimposed uncoated cell and cell coated with  $0.093 \text{ mg/cm}^2$  gold. Major peak from uncoated cell (lower) is Cl, with P and Si peaks to the left. Logarithmic vertical scale.

the coating. In order to avoid beam drift off the cell, we visually monitored the SEM display during analysis. The square scanned raster (one frame per sec.)<sup>1</sup> was kept centered on the cell during this time. Beam diameter was of the order

<sup>1</sup>A slow scan rate was used to avoid the dwell time at the edge of the raster common to TV sweep rates, which would produce undesirable weighting of the data.

of  $0.8 \mu\text{m}$ . Subsequent wavelength scans on samples of coating materials, Figs. 1 & 2, and x-ray intensity measures were performed at 10 times the sample current used for cell analyses, to assure the absence of interferences from our measurements. This data is reported as Au residual in Table 1. Calibration standards were minerals and metals, although we intend to examine biological standard materials. Table 1 lists data pertinent to the spectrometers and calibrations.

We generated energy dispersive spectra with samples of coating metals, gold and

gold/palladium, and with coated and uncoated erythrocytes, Figs. 3 and 4. These spectra indicate the interferences caused by the coating materials with the elements which are of interest to this study.

Biological quantification schemes using peak/background ratios are not directly applicable to this work since most of our background is produced by the coating. Based on observed intensities for coating elements, we calculated a mass-thickness of the coating for each cell using a thin-film on substrate program

(McCarthy and Wodtke, 1977; Yakowitz and Newbury, 1976) available on our instrument. This mass-thickness was then used to determine a transmitted fraction (Cosslett and Thomas, 1964a) for those electrons which penetrate the coating, and the attenuation of x-rays emerging.

At present, we leave the production of x-rays within the cellular materials in a semi-quantitative state. Table 2 presents results corrected only for the transmitted fraction of electrons and the attenuation of x-rays. We report dry mass-fraction of the elements. Table 3 lists our corrections.

TABLE 2: ELEMENTAL ANALYSES FOR CELL TYPES AND TISSUE MATRICES

HYPERTROPHIC SCARS	k Ratio [1]		kc/ZAF[2]		(fraction $\times 10^4$ ) $\pm 1\sigma$	
	Au	Pd	Fe	P	Ca	S
Erythrocytes x values of H.S.(9)	.532		4.6 $\pm$ 1	8.8 $\pm$ 1	3.1 $\pm$ 1	79 $\pm$ 1
Erythrocytes (Std.).229 (x of 16)			3.4 $\pm$ 0.3	3.3 $\pm$ 0.3	1.3 $\pm$ 0.2	19 $\pm$ 1
Type I Cells	.091 .106 .106	.054 .062 .062	4500 $\pm$ 45 6800 $\pm$ 20 5600 $\pm$ 56	9 $\pm$ 1 220 $\pm$ 2 19 $\pm$ 1	8 $\pm$ 1 10 $\pm$ 1 2 $\pm$ 1	27 $\pm$ 1 13 $\pm$ 2 *
Type II Cells	.59 .72 .153 .60 .52	.080	11 $\pm$ 3 8 $\pm$ 4 60 $\pm$ 2 20 $\pm$ 3 7 $\pm$ 2	10 $\pm$ 1 23 $\pm$ 2 53 $\pm$ 3 17 $\pm$ 1 41 $\pm$ 2	10 $\pm$ 2 4 $\pm$ 2 16 $\pm$ 1 15 $\pm$ 2 14 $\pm$ 2	106 $\pm$ 2 200 $\pm$ 4 81 $\pm$ 2 120 $\pm$ 1 95 $\pm$ 2
Myofibroblast (2)	.091 .091	.054 .054	14 $\pm$ 1 12 $\pm$ 1	4 $\pm$ 1 10 $\pm$ 1	1 $\pm$ 1 1 $\pm$ 1	50 $\pm$ 1 61 $\pm$ 1
Scar matrix (4)	.091 .70 .44 .60	.054	1 $\pm$ 1 2 $\pm$ 3 3 $\pm$ 2 35 $\pm$ 3	44 $\pm$ 1 22 $\pm$ 2 11 $\pm$ 1 27 $\pm$ 2	1 $\pm$ 1 2 $\pm$ 2 4 $\pm$ 1 10 $\pm$ 2	68 $\pm$ 1 120 $\pm$ 3 77 $\pm$ 2 128 $\pm$ 3
DEVELOPING DEER ANTLER						
Chondrocyte (4)	.82 .82 .78 .85		0 $\pm$ 6 0 $\pm$ 6 0 $\pm$ 7 8 $\pm$ 7	358 $\pm$ 5 539 $\pm$ 5 198 $\pm$ 33 151 $\pm$ 14	433 $\pm$ 7 587 $\pm$ 6 574 $\pm$ 98 349 $\pm$ 15	* * 48 $\pm$ 2 62 $\pm$ 5
Myofibroblast (3)	.93 .85 .89		0 $\pm$ 7 0 $\pm$ 7 0 $\pm$ 6	6 $\pm$ 4 36 $\pm$ 3 103 $\pm$ 4	13 $\pm$ 6 38 $\pm$ 5 51 $\pm$ 5	68 $\pm$ 7 93 $\pm$ 7 *
Lacuna matrix (4)	.85 .85 .85 .85		26 $\pm$ 6 0 $\pm$ 6 0 $\pm$ 7 0 $\pm$ 7	682 $\pm$ 7 358 $\pm$ 4 570 $\pm$ 22 297 $\pm$ 10	1148 $\pm$ 11 433 $\pm$ 7 1035 $\pm$ 41 688 $\pm$ 12	* * 61 $\pm$ 3 31 $\pm$ 6

[1] k-ratio is the intensity from the coating compared with that from the bulk standard.

[2] kc/ZAF is the product of c/ZAF for the standard (see Table 1) and the ratio of the intensity from the cell compared to that from the bulk standard, and corrected for transmissions contained in Table 3. This represents an approximation to the mass-fraction contained in the cell. Errors are mostly one standard deviation counting statistics. Unusually large values also include effects of raster shift, which was monitored in recent runs. \*Indicates element not measured.



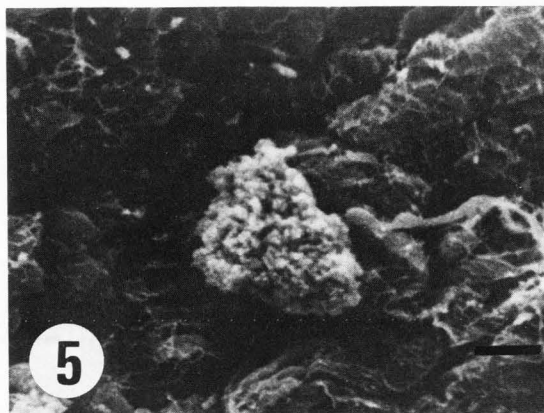


Fig. 5 A Type I cell in the connective tissue of a hypertrophic scar which contained 45% iron. Bar = 5 $\mu$ m.

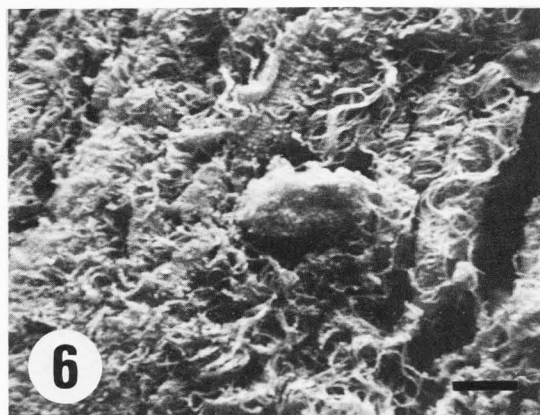


Fig. 6 A Type II cell in connective tissue matrix of hypertrophic scar. This cell demonstrated low iron, phosphorus and calcium, but relatively higher sulfur values. Bar = 5 $\mu$ m.

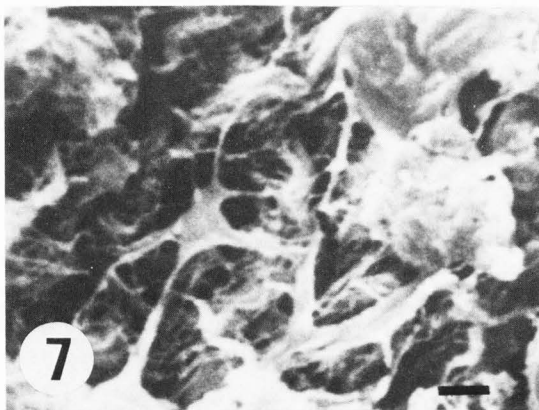


Fig. 7 Cell in matrix of hypertrophic scar regarded as myofibroblast. Bar = 5 $\mu$ m.

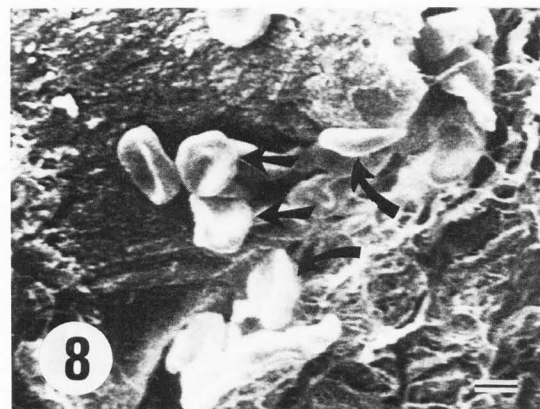


Fig. 8 Extravasated erythrocytes (arrows) in connective tissue of keloid used as in situ control. Bar = 5 $\mu$ m.

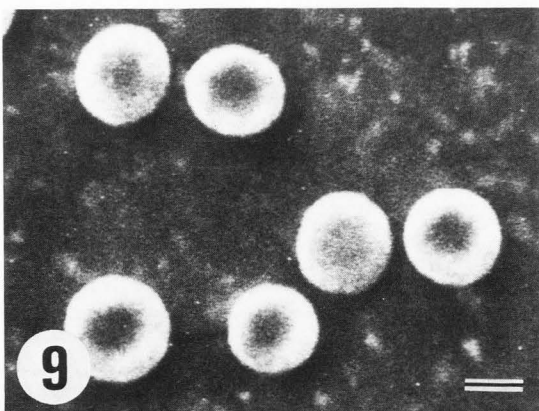


Fig. 9 Erythrocytes placed on spectrographically-pure carbon platform for control study. Bar = 5 $\mu$ m.

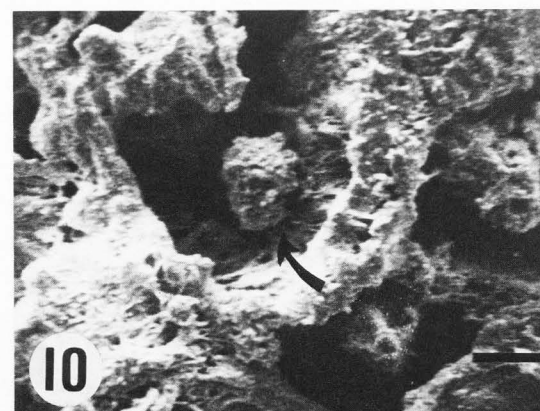


Fig. 10 Cell (presumably chondrocyte) ( $\rightarrow$ ) in lacuna of mineralizing matrix of developing deer antler. Bar = 5 $\mu$ m.

### Results

Elemental values for cells studied in the scar tissues and normal skin enabled us to clearly discriminate between two general connective tissue cell types, Type I and Type II cells (Table 2). Type I cells contained an unusually high content of iron. These cells may have a highly variable morphology, some smooth surfaced and essentially round, others appearing angular with surface variations (Fig. 5). Their phosphorus levels may be variable but calcium and sulfur values are low.

Type II cells (Fig. 6) have unremarkable values for iron, phosphorus or calcium, but relatively high values for sulfur (Table 2).

The cells suspected as being myofibroblasts in the scar tissues (Fig. 7) demonstrate low values for all four elements tested.

The connective tissue matrix in the scar

tissue was also analyzed. Elemental values for iron, phosphorus and calcium were all essentially low, but relatively high sulfur data were recorded. It may also be noteworthy that in one case for scar matrix an increased value for iron was obtained which seemed to differ from the other matrix tests.

Typically biconcave disc-shaped erythrocytes were easily identified in the test tissues (Fig. 8). Because their values for iron at first seemed low, we obtained fresh blood, and examined these erythrocytes placed on a spectrographically-pure carbon platform (Fig. 9). The values obtained from these cells, given in Table 2, are also quite low in all elements, especially in iron ( $x=3.4 \pm 0.3$ ).

Using the regenerating deer antler as a control for nucleated cells (Fig. 10, chondrocyte) we obtained a level of phosphorus

TABLE 3: EFFECT OF COATING ON ELEMENTAL ANALYSES

	Au		Pd		Transmission			
					e <sup>-</sup>	x-ray		
	k	et	k	et		Fe	P	Ca S
HYPERTROPHIC SCARS								
Type I cells (3)	.091	.049	.054	.032	.72	.96	.88	.85 .78
	.106	.055	.062	.036	.70	.96	.86	.83 .76
	.106	.055	.062	.036	.70	.095	.84	.80
Type II cells (5)	.59	.19	--		.40	.91	.74	.68 .45
	.72	.23	--		.30	.90	.69	.63 .38
	.153	.074	.080	.044	.62	.94	.82	.78 .70
	.60	.19	--		.40	.91	.74	.68 .45
	.52	.17	--		.45	.92	.76	.71 .49
Myofibroblast (2)	.091	.049	.054	.032	.72	.96	.88	.85 .78
	.091	.049	.054	.032	.72	.96	.88	.85 .78
Scar Matrix (4)	.091	.049	.054	.032	.72	.96	.88	.85 .78
	.70	.22	--		.33	.90	.70	.64 .40
	.44	.15	--		.48	.93	.79	.74 .54
	.60	.19	--		.40	.91	.74	.68 .45
DEVELOPING DEER ANTLER								
Chondrocyte (4)	.82	.26	--		.25		.66	.60
	.82	.26	--		.25		.66	.60
	.78	.25	--		.28	.89	.67	.61 .35
	.85	.28	--		.22	.88	.64	.57 .31
Myofibroblast (3)	.93	.30	--		.20	.87	.62	.55 .29
	.85	.28	--		.22	.88	.64	.57 .31
	.89	.29	--		.21	.88	.63	.56
Lacuna matrix (4)	.85	.28	--		.22	.88	.64	.57
	.85	.28	--		.22	.88	.64	.57
	.85	.28	--		.22	.88	.64	.57 .31
	.85	.28	--		.22	.88	.64	.57 .31
Collagen matrix (1)	.75	.24	--		.30	.89	.68	.62 .37

k is the k-ratio from Table 2. et is the mass thickness in the film computed from k. e<sup>-</sup> is the electron transmission through the coating film. The right-most four columns are the x-ray transmissions.

which we hoped would serve as a guide for an expected level in the fibroblast. Yet, the phosphorus level as well as that for calcium was quite high while iron levels were essentially zero and sulfur levels low.

Myofibroblasts would be predictably difficult to find in the hypertrophic scar or keloid by SEM because of their unusually extended conformation and small size (Kischer, 1974b). However, these forms appear compatible with what we generally find by transmission electron microscopy. Therefore, again using the developing deer antler, we examined known myofibroblasts (Kischer & Speer, 1982) for each of the four elements. The values obtained from these cells are not consistent.

Elemental measurements were also made on the lacunar matrix of the chondrogenic zone of the developing antler. Except for one case iron levels were not detected while phosphorus and calcium were elevated. Sulfur levels were essentially low.

Because gold, palladium or any metal coating interferes with electron and x-ray passage in and out of the tissue and therefore affects the x-ray intensity of the elements being examined we measured the amount of gold and palladium on the several samples (Table 2). The effect the coating had on the element analysis is shown in Table 3.

As a check for possible interfering x-ray lines, wavelength scans were run in the vicinity of each of the peaks used for analysis of the cell samples. A 100nA current was used, with the beam positioned on bulk samples of the coating materials (Au or Au/Pd) or possible contaminants (Pt, W, Mo). Figures 1 & 2 show data-smoothed results for Fe and P on Au/Pd metal. The scans were made at 6 seconds per point for 200 points. This provided sufficient sensitivity to show potential problems. Figure 2 clearly illustrates the rise in P background (indicated by the vertical lines) caused by the  $Au\ M_{3-5}$  peak to the left. Subsequent measurement provided the negative  $1 \times 10^{-5}$  mass-fraction value reported in Table 1 for the Au residual for P. Additionally, wave length tables were carefully checked for possible interferences. No other problems which would affect this work were found.

#### Discussion

The analysis for iron using WDX on gold coated specimens appears to be useful for distinguishing at least one cell type. Even though the morphology of these cells can be quite unusual the iron content appears to remain high.

The measurements for our two control erythrocytes (in tissue and isolated) assured us the cell type in question is likely not an erythrocyte. The identity of these high iron content Type I cells remains unknown. However, it occurred to us that the only cell type likely to accumulate such vast amounts of iron would be a macrophage. In hypertrophic scars and keloids there is extensive microvascular occlusion. It is likely then that more erythrocytes will die in situ rather than in the spleen. Thus the iron in those cells may remain in the collagenous matrix

until picked up by macrophages. The latter may accumulate this iron over a long time, perhaps years. This may also explain occasional high iron values picked up for matrix measurements.

Type II cells appear to separate from the others on the basis of their high sulfur content. Correspondingly, they show low values for iron, phosphorus and calcium. Again, we cannot identify these cells on the basis of the SEM visual mode. Phosphorus levels are considerably higher than the erythrocytes measured. Therefore, we might assume they are, indeed, a nucleated cell. The higher levels of sulfur would be consistent with a cell in the connective tissue making large quantities of glycosaminoglycans, specifically, chondroitin sulfates. Thus, the most likely candidate for this cell type would be a fibroblast. Indeed, previous studies of the dermal matrix of the hypertrophic scar demonstrate a 14 fold increase in Chondroitin-4-sulfate over that in normal dermis.

Conclusive evidence for the identification of these cell types may be obtained by future studies including transmission electron microscopy.

Myofibroblasts are difficult to find visually in the SEM, but once found they are not difficult to identify. However, one of the problems in attempting to differentiate myofibroblasts by elemental values is the fact that these cells are stretched out, spider-like; therefore, the cell thickness is probably not more than about 2 micrometers. The % element concentration would be appropriately diluted by wave lengths generated from underneath the cell from the matrix.

The use of cells and matrix in the developing deer antler as quasi controls is only partially valuable. Phosphorus and calcium are elevated for the chondrocyte and the chondrocytic lacunar matrix. Mineralization occurs rapidly in this tissue and does so in the presence of low chondromucoids. The presence of relatively low sulfur is another indication that use of this tissue provided good guidelines for elemental analysis. Mineralization also occurs within the cell (chondrocyte). Thus the higher phosphorus level no doubt reflects the mineralizing process and thus would mask a phosphorus level reflecting normal nuclear values.

The thicker gold coating might be expected to compromise the values of some of the elements. The more absorption of electrons the greater reduction in x-ray intensities. Yet in our specimens which had the thickest gold coating (deer antler) the measured ratio of calcium to phosphorus (expected to be about 1.8 to 2.0) was very close to the predicted value and thus calcium and phosphorus seemed unaffected.

We have presented our data as dry mass fractions rather than in biologically more sensible units because this more directly relates to the state in which we find our cells. We have attempted to retrieve chemical data from samples which were originally prepared with no thought given to subsequent microanalysis. We



TABLE 4: MONTE CARLO DERIVED CORRECTIONS

Emitted Intensity Ratio: coated sample/bulk pure element: 15kV: Au metal coating: .0001 concentrations

Coating Thickness mg/cm <sup>2</sup>	Na	P	S	K	Ca	Fe
0.0*	.780	1.000	1.034	.981	.994	.850
0.1	.177	.204	.148	.196	.162	.130
0.2	.043	.083	.044	.068	.058	.054

\*Traditional ZAF calculation.

Monte Carlo calculations from NBS. (Myklebust, personal communication)

have left the attempt at quantification of the x-ray production in the cellular material for future work. Use of biological standard materials will help. There is partial compensation occurring in that the electrons entering the cellular material have been extensively scattered in passing through the coating, and thus produce their ionizations earlier on. This tends to offset the few keV of energy loss experienced in the coating. Monte Carlo computer analysis for this situation would be helpful, and preliminary calculations have been performed (Myklebust, personal communication, 1984). Table 4 presents the results of this calculation, based on a simple model of the cell as a flat piece of carbon with specified gold coating thickness, 0.1 and 0.2 mg/cm<sup>2</sup> and trace levels of the elements of interest. We are comparing these results with measurements performed on coated and uncoated erythrocytes, but none of this is made use of here. We present Table 4 at this time because of its uniqueness and possible use to other workers. We gratefully acknowledge the National Bureau of Standards for performing the Monte Carlo calculations for us.

No attempt has been made to examine possible mass loss in this work. We have used dosages in the range of 10 to 200 coulombs/cm<sup>2</sup>. The metallic coating certainly tends to protect the cellular material.

#### References

1. Anderson, CA, (1966). Electron probe microanalysis of thin layers and small particles with emphasis on light element determination. In: The Electron Microprobe, TD McKinley, KFJ Heinrich, and DB Wittry, Eds., Wiley, New York, p. 58.
2. Anderson, CA, (1967). The Quality of X-Ray Microanalysis in the Ultra-soft X-Ray Region, Brit. J. Appl. Phys., 18:1033-1043.
3. Anderson, CA and Hasler MF, (1966). Extension of electron microprobe techniques to biochemistry by the use of long wave length X-rays. Proc. 4th Int. Cong. on X-Ray Optics and X-Ray Microanalysis, Orsay, Herman, Paris, pp. 310-327.
4. Beaman, DR and Isasi, JA, (1972). Electron Beam Microanalysis, Am. Soc. for Testing and Materials, STP 506, p. 56.
5. Bessis, M (1973). Living Blood Cells and Their Ultrastructure. Springer-Verlag, New York, pp. 85-180.
6. Cosslett, VE, Thomas, RN (1964a). Multiple scattering of 5-30 keV electrons in evaporated metal films., I. Total transmission and angular distribution. Brit. J. Appl. Phys., 15:883-907.
7. Cosslett, VE, Thomas, RN (1964b). Multiple Scattering of 5-30 keV Electrons in Evaporated Metal Films., II. Range-Energy Relations., Brit. J. Appl. Phys., 15:1283-1300.
8. Kischer, CW (1974a). Collagen and dermal patterns in the hypertrophic scar. Anat. Rec., 179:137-146.
9. Kischer, CW (1974b). Fibroblasts of the hypertrophic scar, mature scar and normal skin: a study of scanning and transmission electron microscopy. Tex. Rpts. Biol. Med., 32:699-710.
10. Kischer, CW, Shetlar, MR, Shetlar, CL (1975). Alterations of hypertrophic scars induced by mechanical pressure. Arch. Dermatol., 111:60-64.
11. Kischer, CW, Shetlar, MR (1979). Microvasculature in hypertrophic scars and the effects of pressure. J. Trauma, 19:757-764.
12. Kischer, CW, Speer, DS (1982). Developing antler as a model system of fibrillogenesis. 40th Ann. Proc. Elect. Microsc. Soc. Amer. Bailey, G.W. Ed., Claitors Publishing Division, Baton Rouge, p.298-299.
13. Makita, T (1981). X-Ray microanalysis of the avian shell gland and eggshell. Scanning Electron Microsc. 1981; II:473-480.
14. McCarthy, J, Wodtke, N (1977). Thin Film on Substrate (TFSS) Program Description, NS-885-F, Tracor Northern, Inc., Middleton, WI 53562.

15. Reed, SJB, (1966). Spatial Resolution in Electron Probe Microanalysis, Proc. 4th Int. Cong. on X-Ray Optics and X-Ray Microanalysis, Orsay, Herman, Paris, p. 339.
16. Roomans, GM, Shelburne, JD, eds. (1983). Basic methods in Biological x-ray Microanalysis. SEM, Inc., AMF O'Hare, IL.
17. Yakowitz, H, Newbury, DE (1976). A Simple Analytical Method for Thin Film Analysis with Massive Pure Element Standards. Scanning Electron Microsc. 1976; I:152-162.

#### Discussion with Reviewers

B. Forslind: At analysis of cells in your bulk specimens can you be sure that your excitation volume does not include some of the underlying matrix especially when the thin myofibroblasts are the objects?

Authors: No. In fact, we do suspect we are obtaining some data from under the myofibroblasts in the scar tissue. They are thin enough across the cell body that it seems unlikely we could characterize the cell on an elemental basis at this time.

B. Forslind: It appears to me that in the present study only erythrocytes could be distinguished from other cell types. Could you suggest any type of "marker" suitable for introduction into connective tissue cells to allow identification of such cells on a cell type basis?

Authors: Yes, but if one is referring to introducing a marker into human connective tissues prior to obtaining the tissue for study, legal restrictions may prevail. However, to find a suitable model for Type I cells which seem to accumulate such a high quantity of iron, one might test the ability of macrophages to do so from experimental animal tissue studies. For example, one might inject an iron product (IP) into a rat and subsequently collect macrophages and test their iron levels. One might also feed cultures of macrophages to the same end. The same approach might be said for studying fibroblasts in culture, especially those actively synthesizing chondroitin sulfates (testing for sulfur).

G.M. Roomans: Is your spatial resolution sufficient to distinguish chondrocytes from lacuna matrix?

Authors: Yes, in most cases. The diameter of the chondrocyte within the lacuna is of the order of 7 to 8  $\mu\text{m}$ . Therefore, data we obtain from the chondrocyte is highly unlikely to be also coming from the lacunar matrix.

G.M. Roomans: Can erythrocytes and fibroblasts be completely distinguished from the matrix?

Authors: In the case of erythrocytes, usually. In the case of fibroblasts, it is often difficult. Because of the variable topography of the cut face of the dermal matrix, fibroblasts blend in exceedingly well with the connective tissue. By SEM it is often difficult to pick them out. This usually must be done at about 800X magnification or above.

G.M. Roomans: It has been shown by Boekestein et al. SEM/1983/II:725-736, that there are a number of problems with the ZAF correction as applied to biological tissue. How are these handled in your work?

Authors: We do not make use of ZAF corrections for our cell analyses. The ZAF we use is applied only to the measurements on our mineral standards, for which that technique has been proven.

G.M. Roomans: This paper shows that erythrocytes could be identified by their Fe content. In principle, this could also be done by EDX and not necessitate mounting WD detectors on the microscope. Since apparently EDX facilities were available on your instrument, have you carried out EDX analysis on your material?

Authors: We have performed EDX analyses on our tissues. There is no interference from gold or palladium lines with iron analyses. But as Figure 4 shows there is interference with phosphorus and sulfur, two of the elements in which we were interested. As can be seen from the same figure the gold coating on the cell significantly raises the x-ray continuum. This puts EDX at a further disadvantage in terms of the limit of detectability even though there may not be any interfering lines.

The instrument we used already has wave length detectors mounted on it. Therefore, it required no extra energy to change from one method of analysis to another.

Reviewer #3: A typical SEM sample has an extremely rough surface, quite different from the polished flat surface, normal to the electron beam that should be used for an electron microprobe sample in the ARL-SEM-Q. How do you simultaneously present to the electron beam and the various spectrometers an appropriate face of the SEM samples?

Authors: We were not concerned with the overall sample surface. The SEM image of a cell is as viewed along the electron beam. By centering the raster on what looks on the screen to be the top of the cell we put the raster on the top of the cell itself. Assuming that the cell is reasonably symmetrical we are treating the different spectrometers reasonably alike. We do not measure cells that are obviously tilted, nor those which might be obscured by their surroundings.

Reviewer #3: Most investigators report an apparent, substantial, rapid loss of sulfur signal from dried biological tissue sections analyzed at room temperature. The losses, which may account for 50% or more of the S signal occur with an electron dose much less than required for a typical data collection interval. Is bulk dried tissue different? Are S counting rates stable with time in your samples?

Authors: We performed repeated 50 second counts and found no systematic change for any of the elements. This may not be surprising since the literature indicates that changes usually occur in a shorter dosage time than this.

Reviewer #3: Conventional SEM preparative techniques remove most electrolytes from biological soft tissue, the preparation may not deplete hard tissues (antlers) of Ca, but what of cells? Have you determined whether or not your preparation faithfully preserves Ca in soft tissues?

Authors: No we have not. Indeed, we have not determined the effect of fixation or tissue processing on any of our tissues. However all of the tissues studied (with the exception of the erythrocyte standard samples) were fixed in the same identical way. All were fixed and processed as detailed in the Materials and Methods.

The effect of fixation with respect to how elemental content is affected is undoubtedly important, but requires a complete separate study. If one proposes that certain elements are lost or depleted significantly by fixation, then finding high levels of such elements suggests that even higher levels were originally present, rendering the measured values, all the more significant.

One might assume that 1) all cell types would be affected by fixation in the same way. Finding reasonable levels for some elements would still enable a differentiation of cell types; 2) elemental loss would be different in different cell types. This would, in fact, actually help to differentiate the cell types. Information relative to absolute element loss would not be obtained, but we still would have a comparative base by which separation could be made; 3) elemental loss through fixation (assuming No. 2 would be the case) might be such that different cell types with different contents of certain elements would lose dissimilar amounts so that they eventually would look to be the same cell type by microprobe analysis. This is unlikely to be the case, though, for more than one or two elements.

Reviewer #3: Anderson (1966) has shown that using 15 keV the electron spread in low density material might exceed 20  $\mu\text{m}$ . Have you determined your analytical resolution?

Authors: No. This is a very difficult question due to variable topography and coating thickness. Using the data of Anderson and Hasler (1966) as presented by Anderson (1967) we estimate the volume of x-ray production to range from 100 to 500  $\mu\text{m}^3$  (for  $\text{ZnK}\alpha$  and  $\text{NaK}\alpha$ , respectively) for 15 keV and density 0.42g/cm<sup>3</sup>. This corresponds to spherical diameters of 6 to 10  $\mu\text{m}$ . These are on the order of our cell sizes. Other data from Anderson (1967) computes as 17  $\mu\text{m}$  maximum and 8  $\mu\text{m}$  mean depth for x-ray production. Even worse estimates obtain using data of Reed (1966) as presented by Beaman and Isasi (1972). For  $\text{FeK}\alpha$  we find 5  $\mu\text{m}$  qualitative resolution, with 99% of the x-rays produced in a 22  $\mu\text{m}$  diameter region!

These numbers are for uncoated cells; coating helps resolution by lowering the electron energy which produces a substantial reduction in excitation volume. The gold coating on our samples range from .08 to .30 mg/cm<sup>2</sup>. From the data of Cosslett & Thomas (1964b) we find mean energies in the cell of 14 - 11 keV. This effect reduces the excitation range by as much as a factor of 2 for  $\text{FeK}\alpha$ . Thus, we have resolution in the range 3 to perhaps 8  $\mu\text{m}$ . Excitation of neighboring regions on the sample will be further reduced by the additional electron energy loss in exciting the cell, due to an additional passage through the coating. In the future, we should fine-tune our operating voltage for better resolution without losing too much  $\text{FeK}\alpha$  excitation.